ADVANCES IN SIMULATING TOKAMAK TURBULENT TRANSPORT

G.W. Hammett, M.A. Beer, J.C. Cummings, W. Dorland[1],
W.W. Lee, H.E. Mynick, S.E. Parker, R.A. Santoro,
M. Artun[2], H.P. Furth, T.S. Hahm, G. Rewoldt, W.M. Tang
Princeton Plasma Physics Laboratory, Princeton, NJ 08543 USA
[1]Institute for Fusion Studies, Austin, TX 78712 USA
[2]University of California at Los Angeles, CA USA

R.E. Waltz, G.D. Kerbel[†], J. Milovich[†]
General Atomics, P.O. Box 85608, San Diego, CA 92186 USA
[†]NERSC at Livermore National Laboratory, Livermore, CA 94550 USA

Abstract

Much progress has been made in simulating tokamak turbulent transport using both gyrofluid and gyrokinetic particle techniques. Recent simulations have focused on Ion Temperature Gradient (ITG) driven electrostatic turbulence, a potential candidate for explaining turbulence in some parameter regimes, and have explored experimentally-relevant physics issues such as the long-wavelength peak in measured spectra, the important role of sheared flows in turbulence, and the scaling of the transport with normalized gyroradius ρ_i/a and other parameters.

This paper presents the first nonlinear gyrofluid simulations which simultaneously include trapped-electron effects (for arbitrary collisionality) as well as the ion temperature gradient drives, in 3-D toroidal simulations capable of high resolution. This enables more realistic comparisons with experiments, and provides the full transport matrix (of electron and ion heat and particle fluxes), so that such issues as particle pinches or convection multipliers can be investigated. A relatively sophisticated trapped-electron model is used which retains pitch-angle dependence throughout. This is potentially important for advanced tokamak regimes (negative shear, second stability) where a major fraction of the trapped particles have favorable drift. We also present initial linear results including the passing electron fluid equations needed to get fully electro-magnetic fluctuations (i.e., "finite β" effects which introduce coupling between drift-like and MHD-like modes) to look for a possible β dependence of the transport.

1. Introduction

Turbulent transport in tokamaks is a very challenging scientific problem. It is an intrinsically nonlinear, chaotic, 3-dimensional (plus velocity space) problem involving a wide range of space and time scales. It is further complicated by a zoo of instability driving mechanisms, and by puzzling experimental results exhibiting

a number of different regimes. Computer simulations are a valuable tool in tackling these problems, in combination with analytical insights and detailed comparisons with experiments. Our goal is to develop quantitative predictions of tokamak turbulence that we can compare with present experiments, and then use to aid the design of future fusion reactors. Fairly good agreement between experiments and nonlinear ITG turbulence simulations was found in the recent work by Dorland et al.[1], providing encouraging evidence that we are on the right track.

The present paper will focus on extending such nonlinear simulations to include more realistic physics, primarily non-adiabatic trapped and passing electrons, to enable more realistic and detailed comparisons with experiments over a wider range of parameters. Trapping in the magnetic well is a robust mechanism for generating the non-adiabatic electrons needed to get electron particle and heat flux. We can now study regimes where the collisionless or dissipative trapped-electron mode (CTEM, DTEM) dominates over the ITG mode, such as in the core of supershots, or mixed regimes where the TEM drive may double the growth rate of the ITG mode. These simulations can also investigate why the cores of supershots are convection dominated with a 3/2 multiplier, or search for possible "off-diagonal" pinch effects. Our quasi-fluid trapped electron model[2] is fairly sophisticated, retaining the full pitch-angle dependence throughout. We also present initial linear results including the passing electron fluid equations needed to get magnetic fluctuations, $\delta A_\parallel$ as well as $\delta\Phi$. A number of other physics results from the gyrofluid and gyrokinetic codes will also be described, including the issue of Bohm vs. gyro-Bohm scaling.

2. Gyrofluid Simulation Developments

"Gyro-Landau fluid" (or gyrofluid) equations are an extension of the usual fluid equations to include models of kinetic resonances and gyro-averaging (FLR) which play important roles in fusion plasma turbulence. They are essentially a reduced set of moments of the gyrokinetic equation which include models of parallel kinetic resonances (Landau-damping)[3], linear and nonlinear gyro-averaging (FLR) effects[4], toroidal drift resonances (first with 4 moments[5] and now with 6 moments including magnetic mirroring effects[2, 6]). They have been extended[7] to multiple ion species (such as D/T/beams/impurities, including ion-ion collisions), an important capability needed for realistic comparisons with actual experiments. Extensions to trapped electrons[2] and passing electrons[8] are discussed below. There are some nonlinear regimes where the gyro-Landau fluid approximations break down (i.e., they require many terms to converge), as pointed out by Mattor[9] for ion Compton scattering in the low-frequency, weak-turbulence regime, $\gamma \ll \omega \ll k_\parallel v_{ti}$. However, the gyrofluid approximations should work fairly well in the strong-turbulence regimes expected in tokamaks (more details on these justification issues can be found in Ref.[10, 6, 11]). Non-

linear benchmarks between gyrofluid and gyrokinetic codes have been carried out and find similar behaviors in regimes tested so far[10, 12, 13].

One of the interesting nonlinear results observed in the gyrofluid ITG simulations is that the turbulence often generates strong sheared flows ($n = 0$ "radial modes") which can in turn control the saturation of the turbulence[10, 6, 14, 15]. These generated sheared flows appear to be less important when the magnetic shear is high[7, 16]. The importance of self-generated flows in edge turbulence and H-modes has been previously emphasized[17, 18], while the present work shows how it can be important in core ITG turbulence as well. Nonlinear gyrofluid studies have found[14] that when the shearing rate associated with the $E \times B$ flow, $\gamma_E = (r/q)\partial(V_\phi/R)/\partial r$, exceeds the maximum growth rate of the microinstabilities, then the turbulence is suppressed. Including the parallel flow shear which drives the Kelvin-Helmholtz instability tends to prevent complete stabilization. Increasing rotational shear is a leading candidate for explaining the VH improved confinement regime on DIII-D.

3. Quasi-Fluid Bounce-averaged Trapped Electrons

Here we outline the derivation of a "quasi-fluid" treatment of trapped electrons, and present initial nonlinear results. Details of the derivation and results will be found in Ref.[2]. Since we are interested in time scales much longer than the electron bounce frequency, we start with the nonlinear bounce-averaged drift-kinetic equation [19]:

$$\left(\frac{d}{dt} + i\langle\omega_{de}\rangle_b\right)\langle f_e\rangle_b = \langle C\rangle_b\left(\langle f_e\rangle_b - \langle\Phi\rangle_b\right) - iF_M(\omega_{*e}^T - \langle\omega_d\rangle_b)\langle\Phi\rangle_b$$

$$f_e = F_M(\Phi - \langle\Phi\rangle_b) + \langle f_e\rangle_b$$

where $\langle ...\rangle_b$ denotes bounce-orbit averaging. Φ has been normalized to e/T_e and $d/dt = \partial/\partial t + \hat{b} \times \langle\Phi\rangle_b \cdot \nabla$. The nonlinear $\mathbf{E} \times \mathbf{B}$ terms (in d/dt) have the same form as for ions, except that y is now thought of as a toroidal coordinate, i.e., radial $\mathbf{E}$ causes toroidal precession of trapped electrons. Also, only the bounce-averaged Φ enters the $\mathbf{E} \times \mathbf{B}$ drifts. Bounce averaging eliminates the parallel direction, so $\langle f_e\rangle_b(x, y, E, \kappa)$ is a function of radius, x, toroidal angle, y, energy, $E = mv^2/2$, and pitch angle κ.

We take moments over $(v_\perp, v_\parallel)$ of the gyrokinetic equation to get our 3-D gyrofluid equations, but we only need to take moments over energy of the bounce averaged kinetic equation to get 3-D trapped-fluid equations for the electrons, which are functions of (x, y, κ), i.e., $n_t(x, y, \kappa) = 4\pi \int_0^\infty dv\, v^2\langle f_e\rangle_b/n_0$, and the higher moments p_t and r_t are similar with additional factors of $v^2/(3v_{te}^2)$ and $v^4/(15v_{te}^2)$ in the integrals. Since $\langle\omega_{de}\rangle_b \propto E$, this introduces the usual closure problem of the coupled moments hierarchy.

$$\frac{dn_t}{dt} \quad + \quad \frac{3}{2}i\omega_{de}p_t - \frac{3}{2}i\omega_{de}\langle\Phi\rangle_b + i\omega_{*e}\langle\Phi\rangle_b = \langle C\rangle_b(n_t - \langle\Phi\rangle_b)$$

$$\frac{dp_t}{dt} + \frac{5}{2}i\omega_{de}r_t - \frac{5}{2}i\omega_{de}\langle\Phi\rangle_b + (1+\eta_e)i\omega_{*e}\langle\Phi\rangle_b = \langle C\rangle_b(p_t - \langle\Phi\rangle_b)$$
$$\frac{dr_t}{dt} + \frac{7}{2}i\omega_{de}t_t - \frac{7}{2}i\omega_{de}\langle\Phi\rangle_b + (1+2\eta_e)i\omega_{*e}\langle\Phi\rangle_b = \langle C\rangle_b(r_t - \langle\Phi\rangle_b)$$

We use an extension of the Landau-fluid closure approximation[3] to provide a 3-pole model of the precession resonance and phase-mixing, $t_t = -i\frac{|\omega_{de}|}{\omega_{de}}(\nu_a n_t + \nu_b p_t + \nu_c r_t)$, where each closure coefficient has both a dissipative and nondissipative piece, $\nu = \nu_r + i\nu_i|\omega_{de}|/\omega_{de}$, but now ω_{de}, the bounce averaged ∇B and curvature drift frequency (the toroidal precession frequency) is pitch angle dependent. The closure coefficients are chosen to match the linear kinetic response: $\nu_a = (-.071, -.290)$, $\nu_b = (-.689, 1.102)$, and $\nu_c = (1.774, -.817)$. Retaining the pitch angle (κ) dependence of the trapped-electron fluid "density", $n_t(x, y, \kappa)$, "pressure", etc., is needed to represent the pitch-angle dependence of $\langle\omega_{de}\rangle_b$. This recovers the favorable drifts of barely-trapped particles, and is potentially important for Advanced Tokamak regimes involving negative-shear or second-stability. It also allows use of an actual diffusive pitch-angle-scattering operator in the "fluid" equations (better handles trapped-passing boundary layer effects), whose bounce-average is calculated in Ref.[20]. Note that $\langle C\rangle_b$ operates on $\langle\Phi\rangle_b$ which depends on pitch-angle, and the collision operator causes the net f_e to relax to adiabatic limit when $\nu_{\text{eff}} \gg \omega$. The energy dependence of the pitch-angle scattering operator will couple different energy-moments together, though for now we have assumed $\nu_\perp(E) \approx \nu_0$ for simplicity. The real space electron density (normalized to n_0), which is needed to calculate the potential, is related to the pitch-angle-dependent trapped electron density by (in the large aspect ratio limit):

$$n_e(x, y, \theta) = \int d^3v f_e = \Phi + \sqrt{2\epsilon}\int_{\sin(\theta/2)}^{\kappa_{max}} \frac{d\kappa\,\kappa[n_t(x, y, \kappa) - \langle\Phi\rangle_b(x, y, \kappa)]}{\sqrt{\kappa^2 - \sin(\theta/2)}},$$

where θ is the coordinate along the field line. The lower bound on the κ integral arises since only electrons with their turning points, θ_t, beyond θ contribute to the local density, and $\kappa = \sin(\theta_t/2)$ at the turning point. The integral should go up to the trapped-passing boundary $\kappa_{max} = 1$ for all modes with $k_y \neq 0$ (toroidal mode number $n \neq 0$). However, for toroidally symmetric $k_y = 0$ ($n = 0$) modes one must keep track of the passing particles as well, so the κ integral should extend over all pitch-angles, $\kappa_{max} = 1/\sqrt{2\epsilon_B}$. This is related to the fact that the orbit average $\langle\Phi_n\rangle_b = \langle f_{e,n}\rangle_b = 0$ for passing particles for toroidal mode numbers $n \neq 0$, since Φ_n must vanish as $\theta \to \infty$ for $n \neq 0$, but not for $n = 0$ modes.

This trapped electron model (with the 4+2 moment toroidal gyrofluid equations for the ions) is compared linearly vs. fully kinetic results [21] in Fig. 1A, for $\eta_i = \eta_e = 3$, $q = 1.5$, $\hat{s} = 1$, $L_n/R = 1/3$, $r/R = 1/6$, and $k_\theta\rho = 0.35$ (i.e., parameters as given in Ref.[21]). The kinetic results exhibit a somewhat weaker rate of transition between the collisionless and collisional limits. The gyrofluid

code might be able to reproduce that feature better with an energy-dependent $\nu_\perp$, which will allow higher energy moments to be less collisional.

We present preliminary nonlinear results in Fig. 1B, for the parameters in Fig. 1A, and $\nu_{\rm eff} = 0.1$. For this collisionality, although the linear growth rate nearly doubled, the nonlinear χ_i is close to χ_i from simulations with adiabatic electrons. In the linear stage, the ratio of $\chi_i/\chi_e \approx 7$, which is the quasilinear ratio for the fastest growing mode at $k_\theta\rho \approx 0.4$. Nonlinearly, χ_i/χ_e drops to about 4, consistent with the quasilinear ratio for the peak in the nonlinear spectrum at $k_\theta\rho \approx 0.2$.

4. Finite-β Electromagnetic Gyro-Landau-Fluid Model

ITER-P scaling suggests a χ of the Bohm-like form[22] $\chi \propto (cT/eB)\beta^{1/2}\nu_*^{1/4}$, and the scaling of χ with plasma density (via β) is an important issue for the design of ITER. Thus the extension of turbulence studies to include "finite-β" electromagnetic perturbations is of interest. More details on this extension will be in Ref.[8].

For purely passing particles with no consideration of the mirror force, generalization of the electrostatic GLF model by Waltz, Dominguez, Hammett[5] (WDH) to finite beta is straightforward. We need only include the parallel magnetic vector potential in the parallel momentum equations

$$M_s dU_s/dt = -i\tilde{k}_\parallel(t_s^{-1}P_{\parallel s} + e_s\Gamma_{0s}\Phi) + iM_s e_s\omega_D[(\Gamma_\parallel + \Gamma_\perp)/2U_s - i\sigma_t\mu U_s],$$

$$-\beta_e/2(e_s\partial A_{s1}/\partial t - i\omega_*(1_s A_{s1} + \eta_s A_{s2}))$$

and in all of the fluid equations generalize the $k_\parallel$ operator to $\tilde{k}_\parallel = \hat{b}\cdot\nabla = (\hat{b}_0 + \delta\vec{B}_\perp/B_0)\cdot\nabla$, i.e., including the "magnetic flutter" nonlinearity. This can be expressed in a form similar to the $E\times B$ nonlinearity,

$$i\tilde{k}_\parallel f = ik_\parallel f - (\beta_e/2)\hat{b}_0\times\nabla A\cdot\nabla f.$$

Otherwise the continuity and pressure equations remain unchanged from WDH which may be consulted for notation and further definition. [This section focuses on the "3+1" fluid equations with a reduced FLR model presented in WDH. Other gyrofluid results reported in this paper employ up to "4+2" fluid equations with a more complete FLR model[4], and follow a somewhat different notation.] The same closure coefficients as found in WDH are used to represent parallel and toroidal drift resonances. Φ is determined by the usual gyrokinetic quasineutrality condition, and A is determined by Ampere's law. There are magnetic flutter contributions to the particle and energy fluxes, in addition to the ExB flows and turbulent energy exchange specified in WHD. One can show that Ampere's law forces the magnetic flutter component of the electron and ion

particle fluxes to be the same. The magnetic flutter component of the heat flux is:

$$Q_{Msx} = (3/2)T_{0s}\Gamma_{Mx} - n_{0s}(c_S/a)(\rho_s/a)^2\chi_M dT_{0s}/dr$$

$$\chi_M = (\beta_e/2)^2\sqrt{8/\pi M_s}\Sigma_k|k_\parallel|^{-1}k_y^2 A_k^* \left[A_k - k_\parallel T_{sk}/(\eta_s(\beta_e/2)k_y)\right]$$

This essentially corresponds to magnetic flutter heat flow with the Landau-fluid[3] parallel collisionless diffusivity, $\chi_\parallel = (2/\sqrt{\pi})v_t/|k_\parallel|$ (in physical units). The first term in χ_M represents Rechester-Rosenbluth field line diffusion and the second term is the Kadomtsev-Pogutse back reaction term which prevents significant magnetic heat flow as the field line becomes isothermal $[A_k - k_\parallel T_{sk}$ $/(\eta_s(\beta_e/2)k_y)] \to 0$. Formally, the operator $|k_\parallel|^{-1}$ should be written as $|\tilde{k}_\parallel|^{-1}$, i.e., it should evaluate the phase-mixing due to free-streaming along *perturbed magnetic field lines*. But for now, we are simplifying it to operate along the unperturbed magnetic field. There may be cases where this difference is important, but we believe that the magnetic flutter flows will usually be very small.

We can merge the above equations for passing electrons with a separate set of equations for trapped electrons with some approximations based on dividing velocity space into a trapped region ($|v_\parallel| < \sqrt{\epsilon}v$) and untrapped regions ($\sqrt{\epsilon}v <$ $|v_\parallel| < v$), where $\sqrt{\epsilon} = [(r/R)[1+\cos(\theta)]/[1+(r/R)\cos(\theta)]]^{1/2}$ is the local trapped fraction. These approximations lead to weighting factors of $1 - \sqrt{\epsilon}$ for various terms in the passing electron equations. One must be careful in constructing this model so that the total electron response (passing plus trapped) recovers the proper fundamental limits (such as the adiabatic limit). We have carried out this merger (and carried out successful linear benchmarks) using a somewhat simpler trapped-electron model than presented in the previous section, but we believe the merger of passing and trapped electron "fluid" equations can be carried out with the model of the previous section as well.

The electron equations are stiff in time because the frequency of the waves we want to follow is much lower than the typical electron transit frequency $k_\parallel v_{te}$. To handle this, we use a small-storage, implicit "response matrix" method developed by Kotschenreuther for a gyrokinetic ballooning code[21]. Our finite beta trapped electron code has not yet been run to the nonlinear stage but we believe it gives a satisfactory representation of the linear mode stability in comparison to Kotschenreuther's gyrokinetic stability code. Fig. 2 shows that it reasonably well reproduces the onset of the ideal ballooning mode limit, for the parameters $k_\theta\rho_s = 0.2$, $\hat{s} = 1$, $q = 2$, $a/L_T = 3$, $a/L_n = 1$, $T_i/T_e = 1$, $a/R = 1/3$, and $r/R = 1/6$.

5. Bohm vs. Gyro-Bohm Scaling Puzzles

The scaling of χ with $\rho_* = \rho_i/a$ (i.e., scaling with the size of the tokamak) is a key question of interest for ITER. Though most theories lead to gyro-Bohm-like scalings, $\chi \propto (cT/eB)\rho/a$ (times some function of other dimensionless parameters

independent of ρ_*), dimensionless scaling experiments on TFTR[22, 23] appear to be closer to a Bohm-scaling (χ independent of ρ_*) than a gyro-Bohm scaling.

Cowley proposed[24] using an efficient "minimum-simulation volume" employing field-line coordinates, a concept implemented and elaborated on by others as well ([25, 14, 26]). The main idea is that it should be sufficient to simulate a thin "flux-tube" whose width only needs to be a few decorrelation lengths wide in the directions perpendicular to $\vec{B}$ (while still being very extended along a field line to allow for the long parallel correlation lengths). One should demonstrate the validity of this approach by verifying that the results (the χ and the size of the eddies) are independent of the simulated flux-tube size, once it is larger than a few decorrelation lengths. The simplest versions of this approach ignore the variation of equilibrium parameters (such as $\omega_*(r)$ or $\eta_i(r)$) on the scale of the thin flux tube, and thus implicitly assume a gyro-Bohm scaling.

Detailed convergence studies in flux-tube geometry have been carried out in both gyrofluid[25, 14] and gyrokinetic[16] codes, finding that the results are indeed independent of the simulation size. In essence, these results demonstrate the existence of a gyro-Bohm scaling regime in the limit of $\rho_* \to 0$ (at least for the type of ITG-driven turbulence studied so far). Moreover, these flux-tube simulations (as well as the full-torus simulations[27]) have found that the nonlinear spectrum peaks at a lower $k_\theta \rho$ than the fastest growing linear mode, yielding a spectral width $\Delta k_\perp \rho \sim 0.2$ similar to long-wavelength spectra measured on TFTR[28]. On the other hand, full torus simulations have found a Bohm scaling for χ_i in the smallest range of ρ_*'s which are achievable at present (from $\rho_* = 1/64$ to $1/128$). (Details on these calculations are in the next section and the references therein.) In contrast to the present flux-tube codes, which are effectively scaled to the $\rho_* \to 0$ limit and assume ω_* is constant, this full-torus code includes the radial variation of $\omega_{*T}(r)$, which is presumably affecting the radial correlation lengths of the turbulence to give a Bohm scaling.

These two results can be reconciled by realizing that there may different scaling regimes for different values of ρ_*, as illustrated in Fig. 3. [This figure is meant only as a conceptual illustration and, except for the points from the full-torus results, is not precise.] Present day tokamak experiments lie at ρ_*'s smaller than the full-torus code can reach, and ITER will extrapolate beyond present experiments by another factor of 3. It would seem plausible that future tokamaks with smaller ρ_* will be in more of a gyro-Bohm regime. However, it is not yet proven where the transition between these two regimes lies, or how the transition point scales with other parameters such as T_i/T_e, the closeness to marginal stability $L_{T,crit}/L_T$, the type of instability driving the turbulence, or the presence of sheared flows.

Present dimensionless-scaling experiments[22, 23] appear to be more Bohm-like, though the intrinsically gyro-Bohm model by Dorland et al.[1] wasn't far off. This may be due in part to the ability of marginal stability effects to mask other dependencies in χ (as noted by others also), i.e., χ is sensitive to small changes

in $1/L_{ti}$ if it is near the critical temperature gradient. Indeed the prediction of temperature profiles is much easier in the marginal stability limit where ∇T is determined by the linear $L_{ti,crit}$ rather than the complicated nonlinear physics of χ.

Longer wavelength instabilities can be more sensitive to the variation of $\omega_*(r)$, and analysis of long-wavelength trapped-ion instabilities indeed supports a Bohm-like scaling of ion thermal transport. The stabilizing influence of sheared flows on long-wavelength ($k_r\rho_{bi} < 1$) linear trapped-ion modes has been studied[29] by modifying a two-dimensional code, including full trapped-particle dynamics and poloidal mode coupling. Global modes with radial extent over many rational surfaces can be significantly stabilized by realistic levels of sheared toroidal rotation for TFTR-like parameters. Including a hot beam species turns out to be stabilizing in the absence of rotation, but can have a net destabilizing effect with sufficient rotation. Toroidal rotation effects on shorter wavelength ($k_\theta\rho_i < 1$) toroidal drift modes are studied using the same rotation model in a comprehensive ballooning-representation kinetic calculation[30], and can be stabilizing due to radially local and non-local effects. Analytic studies[31] of sheared-flow effects on turbulence have also been carried out. Earlier cylindrical results have been extended to toroidal geometry including $v_\parallel$ as well as $v_{E\times B}$, finding a scaling on q and $\hat{s}$ which may provide insights into confinement improvement with high triangularity in DIII-D VH modes and the favorable influence of a separatrix or current ramp down.

6. Gyrokinetic Simulation of Tokamak Transport

Fully nonlinear toroidal gyrokinetic equations formulated in the early 1980's[32, 33, 34, 35], have recently become solvable by direct numerical simulation[27] due to enormous gains in computing power and developments in low noise δf methods[39, 40, 41]. For example, simulations of a whole tokamak cross-section with a minor radius of 100-200ρ_i are now feasible on current generation massively parallel supercomputers. These first-principles nonlinear codes have become a vital tool for the improved understanding of anomalous transport.

Global toroidal gyrokinetic simulations have been used extensively to investigate ITG-driven turbulence[27]. The largest runs done so far have been with 8 million particles with a minor radius of $a = 128\rho_i$. Linear results are in reasonable agreement with linear eigenmode calculations[36]. The ensuing turbulent spectrum retains remnants of the linear ballooning mode structure, and peaks at significantly longer wavelengths than the linearly most unstable modes. The k_r, k_θ spectra show features similar to those obtained from recent beam emission spectroscopy and reflectometry measurements on TFTR[28, 37] with the k_θ spectrum peaking at $k_\theta\rho_i \sim$ 0.1-0.2 and the k_r spectrum peaking at zero. By varying the minor radius a/ρ_i from 64 to 128 in the simulation, while keeping all other dimensionless parameters fixed, we have found that the resulting k_r spec-

trum scales as $k_r\rho_s \approx (\rho_i/a)^{1/2}$, while the $k_\theta\rho_i$ spectrum remains fixed. This can easily be shown[38] to be consistent with a Bohm-scaling for χ_i, using a quasi-linear expression for the heat flux and a mixing length saturation level. Fig. 3 shows the measured χ_i vs. a/ρ_i from five runs[39]. All points were measured at the same dimensionless time of approximately $T = 300L_T/c_s$. The $a = 128\rho_s$ run shows an error bar because, in contrast to the other cases, the heat flux did not stay at a steady state at $T = 300L_t/c_s$ but continued to drop until the run was terminated at approximately $T = 1000L_t/c_s$. Work is underway to understand this apparent anomaly. These runs indicate that a transition occurs from a worse-than-Bohm scaling at very small system size ($a/\rho_i < 64$) to a Bohm scaling for larger systems. The scaling of χ_i with the edge safety factor $q(a)$ which is related to current scaling through $I_p \propto 1/q(a)$ is found to be $\chi_i \propto q(a)^{1/4}$. Further discussion on global scaling can be found in Ref. [42]. In addition, global gyrokinetic simulations with artificially narrow variation in the temperature gradient show nonlocal transport in regions where the gradient is zero, indicating $\chi_i \to \infty$ or the break down of local diffusive transport theories. Simulations indicate favorable scaling of χ_i with increasing T_i/T_e.

These global simulations have found $\chi_i \propto |\phi|^2$, suggesting that a weak-turbulence treatment may be appropriate. A greatly reduced description (needing only a modest number of toroidal modes ~ 10) of the essential physics appears to be possible using a set of mode coupling equations with the nonlinear coupling coefficients determined empirically from the simulation itself. Detailed measurements of the nonlinear mode coupling coefficients have been made for the first time[42] which are essential for determining the underlying mechanisms for the downward shift in the wavelength spectrum.

Multi-ion species have been included to investigate their impact on transport. An inward impurity pinch due to ITG microturbulence has been found[43] consistent with recent TFTR experiments[44]. In trace particle simulations, a linear dependence on Z/m for the pinch velocity is observed. We have investigated the thermal transport in the presence of an inverted density gradient in multi-hydrogenic-ion plasmas. In the presence of an inverted density gradient in DT simulations with $\eta_i^T = 4$ and $\eta_i^D = -4$, a factor of 2 increase in χ_i^T has been observed. This increase is related to the "impurity-gradient" instability predicted by Coppi et al.[45], which is a close cousin of the ITG instability, i.e. it is driven by gradients in the average thermal velocity of the ions, but in this case due to gradients in the relative concentrations of light (deuterium) vs. heavy (impurities, or even tritium, relative to deuterium) ions. The tritium experiments on TFTR provide a unique capability for testing various aspects of such D-T-gradient instabilities, which are a topic of interest for understanding fueling in future reactors. Further simulations with different combinations of H, D, and T are in progress.

The global gyrokinetic code has been extended to study the turbulence-generated sheared-flows[46]. Proper treatment[10, 6] of the adiabatic electron

response leads to large self-generated poloidal flows in steady state, with modestly reduced heat transport (at least for TFTR L-mode type parameters). In contrast to local flux-tube gyrokinetic calculations[12, 38, 16], the dominant radial mode is global with $k_r \sim 1/a$, similar to earlier fluid calculations by Hasegawa and Wakatani[47]. Poloidal flow generation via quasilinear radial currents seems to be the most promising theoretical description, which is equivalent to the Reynolds stress argument presented by Diamond and Kim[17]. The effect of toroidal drift orbit averaging on these radial modes is under investigation which will help in validation or improvements in fluid treatments of such modes.

A zero-electron-inertia fluid model has been derived[38, 48] from moments of the drift kinetic equation taking $m_e \to 0$, but with $T_{\|e}$ finite avoiding all accuracy or stability constraints on $k_\| v_{te} \Delta t$, as well as particle noise associated with electron free streaming. This is in the same spirit as previous zero-electron-mass models[49, 50, 51], but the fluid equations are derived from the drift-kinetic equation, and the ions are treated fully gyrokinetic[32, 33]. This approach is a natural extension of both flux tube[12, 38] and whole cross section[27] 3D toroidal gyrokinetic simulations to include effects of electron ExB flow, electron pressure gradient effects (e.g. ω_{*e}), and most importantly the electron parallel current, which in turn is used to include electromagnetic perturbations ($\delta B_\perp$). Work is underway to study the β dependence of χ_i from ITG-driven microturbulence modified by $\delta B_\perp$. The inclusion of finite $\delta B_\|$ is straightforward through the gyrokinetic perpendicular pressure balance equation. Development of an electromagnetic bounce-averaged trapped-electron model is also in progress.

7. Summary

Major steps have been taken towards increasingly realistic physics in tokamak turbulence simulations codes. Here we presented the first nonlinear gyrofluid results including a sophisticated trapped-electron model[2] which retains effects which may be important in advanced tokamak regimes. We applied an extension of the gyrofluid equations to passing electrons to include finite-β electromagnetic perturbations, and tested this linearly. Flux-tube simulation codes (both gyrofluid and gyrokinetic) have demonstrated the existence of a gyro-Bohm scaling regime for ITG-driven turbulence in the limit $\rho_* \to 0$. The full-torus gyrokinetic simulations have found a Bohm scaling at the moderate values of ρ_* computationally achievable at present. There is presumably at transition from Bohm to gyro-Bohm scaling at some intermediate value of ρ_*.

Acknowledgments: We thank Drs. Liu Chen, Steve Cowley, Mike Kotschenreuther, and John Krommes, for valuable insights and discussion. This work is supported in part by the High Performance Computing and Communications Initiative (HPCCI), as part of the Grand Challenge Numerical Tokamak Project, and we are grateful for the use of a Cray C-90 at NERSC (Livermore National Laboratory) and a Thinking Machines CM-5 at the ACL (Los Alamos National

Laboratory). W.D. was supported by a DoE Fusion Postdoctoral Fellowship. This is a report of research sponsored by the U.S. Dept. of Energy under Contract Nos. DE-AC020-76CH03073, DE-AC02-89ER53277, and W-7405-ENG-48; such financial support does not constitute an endorsement by DoE of the views expressed herein.

References

[1] W. Dorland, M. Kotschenreuther, J.Q. Dong, et al., this conference (1994). M. Kotschenreuther et.al., Phys. Plasmas **2**, 2381 (1995).

[2] M.A.Beer, Ph.D. Thesis, (Princeton University, 1994).

[3] G.W. Hammett and F.W. Perkins, Phys. Rev. Lett. **64**, 3019 (1990).

[4] W. Dorland, G. W. Hammett, Phys. Fluids B **5**, 512 (1993).

[5] R. E. Waltz, R. R. Dominguez, and G. W. Hammett, Phys. Fluids B **4**, 3138 (1992).

[6] G.W. Hammett, M.A. Beer, W. Dorland, S.C. Cowley, and S.A. Smith, Plasma Phys. Control. Fusion 35, 973 (1993).

[7] W. Dorland, private communication (1994).

[8] R.E. Waltz, et al., Phys. Plasmas 2, 2408 (1995).

[9] N. Mattor, Phys. Fluids B **4**, 3952 (1992).

[10] W. Dorland, Ph.D. Thesis, Princeton University (1993).

[11] J.A. Krommes and Genze Hu, Phys. Plasmas **1**, 3211 (1994).

[12] S.E. Parker, W. Dorland, R.A. Santoro, et al., Phys. Plasmas **1** 1461 (1994).

[13] R.E. Waltz, B.I. Cohen, M.A. Beer, J.A. Byers, A.M. Dimits, W. Dorland, S.E. Parker, R.A. Santoro, R.D. Sydora, H.V. Wong, "Numerical Tokamak Project Code Comparison", UCRL-ID-117670 (June, 1994).

[14] R.E. Waltz, G.D. Kerbel, and J. Milovich, Phys. Plasmas **1**, 2229(1994).

[15] B. Cohen, T.J. Williams, A.M. Dimits, and J.A. Byers. Phys. Fluids. B **5**, 2967 (1993).

[16] A.M. Dimits, et al., this conference (1994).

[17] P.H. Diamond and Y.B. Kim, *Phys. Fluids B* **3** 1626 (1991).

[18] B.A. Carreras, V.E. Lynch, L. Garcia, *Phys. Fluids B* **3** 1438 (1991)

[19] F.Y.Gang and P.H.Diamond, Phys. Fluids B **2**, 2976 (1990).

[20] J.G.Cordey, Nucl.Fusion, **16**, 499 (1976).

[21] M. Kotschenreuther, G. Rewoldt, and W. M. Tang, Comp. Phys. Comm., **88**, 128 (1995).

[22] F.W. Perkins, et al., Phys. Fluids B **5**, 477 (1993).

[23] S.D. Scott, et al., 14th IAEA, Wurzburg, Germany, September 1992.

[24] S.C. Cowley, R.M. Kulsrud, and R. Sudan, Phys. Fluids B **3**, 2767 (1991).

[25] M.A. Beer, S.C. Cowley, G.W. Hammett, Phys. Plasmas 2, 2687 (1995).

[26] A.M. Dimits, Phys. Rev. E **48**, 4070 (1993).

[27] S. E. Parker, W. W. Lee, and R. A. Santoro, Phys. Rev. Lett. **71**, 2042 (1993).

[28] R. Fonck, et al., Phys., Rev. Lett. **70** 3736 (1993).

[29] M. Artun, Ph.D. Dissertation, Princeton University (1994); M. Artun, in *Proc. of the International Sherwood Fusion Theory Conf.*, March, 1994, Dallas, Texas, oral paper 2E2.

[30] G. Rewoldt, W.M. Tang, and R.J. Hastie, Phys. Fluids **30**, 807 (1987).

[31] T.S. Hahm, Phys. Plasmas **1**, 2940 (1994).

[32] E.A. Frieman and L. Chen, Phys. Fluids **25** 502 (1982).

[33] W.W. Lee, Phys. Fluids **26** 556 (1983).

[34] T.S. Hahm, Phys. Fluids **31** 2670 (1988).

[35] A. J. Brizard, J. Plasma Physics **41** 541 (1989).

[36] W.M. Tang and G. Rewoldt, Phys. Fluids B **5** 2451 (1993).

[37] E. Mazzucato and R. Nazikian, Phys., Rev. Lett. **71** 1840 (1993).

[38] S.E. Parker, et al. in Proc. Joint Varenna-Lausanne Int. Workshop on Theory of Fusion Plasmas, Aug. (1994).

[39] S.E. Parker and W.W. Lee, Phys. Fluids B **5** 77 (1993).

[40] G. Hu and J.A. Krommes, Phys. Plasmas **1** 863 (1994).

[41] A.M. Dimits and W.W. Lee, J. Comput. Phys. **107**, 309 (1993).

[42] H.E. Mynick and S.E. Parker, Phys. Plasmas **2**, 2231 (1995).

[43] R.A. Santoro, PhD Thesis, Princeton Univ. (1993).

[44] P.C. Efthimion, L.C. Johnson, C.H. Skinner et.al., this conference (1994).

[45] B. Coppi, H. Furth, R. Sagdeev, and M. Rosenbluth, Phys. Rev. Lett. **17**, 377 (1967)

[46] J.C. Cummings, W.W. Lee and S.E. Parker, Int. Conf. on Numerical Simulation of Plasmas, Valley Forge, PA, Sept. (1994).

[47] A. Hasegawa and M. Wakatani, Phys. Rev. Lett. **59**, 1581 (1987).

[48] W.W. Lee S.E. Parker, and L. Chen, Int. Conf. on Numerical Simulation of Plasmas, Valley Forge, PA, Sept. (1994).

[49] J.A. Byers, et al., J. Comput. Phys. **27**, 363 (1978).

[50] D.W. Hewett, J. Comput. Phys. **38**, 378 (1980).

[51] B.B. Kadomtsev, and O.P. Pogutse, 10th IAEA Conference, London, **2** 69 (1984).

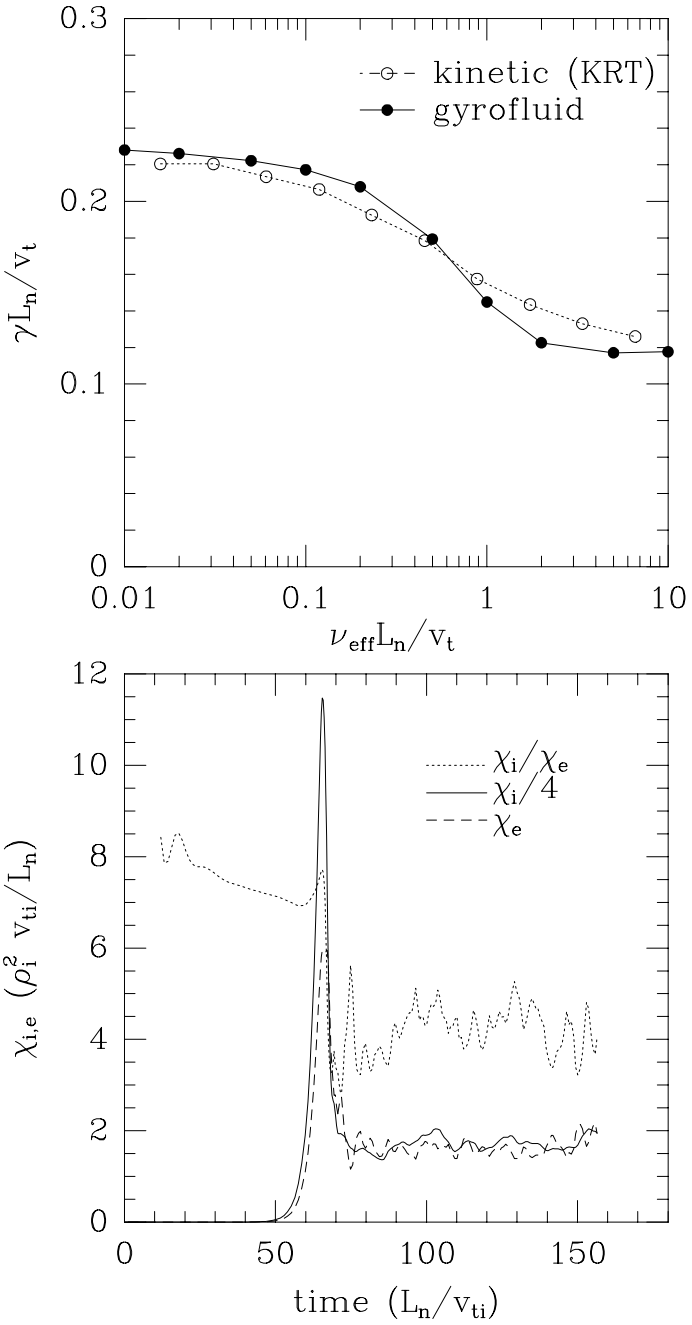

Figure 1: 1A: A comparison of linear growth rates from gyrofluid trapped electron model vs. kinetic theory. As $\nu_{\rm eff}/\omega \to \infty$, the growth rates approach the adiabatic-electron/ITG limit, while for $\nu_{\rm eff} = 0$, trapped electrons increase the linear growth rate by a factor of 2. 1B: Time evolution of χ_i and χ_e from a nonlinear simulation with trapped electrons. The ratio χ_i/χ_e is lower in the fully nonlinear regime ($t > 70$) than it is in the quasilinear regime ($t < 60$).

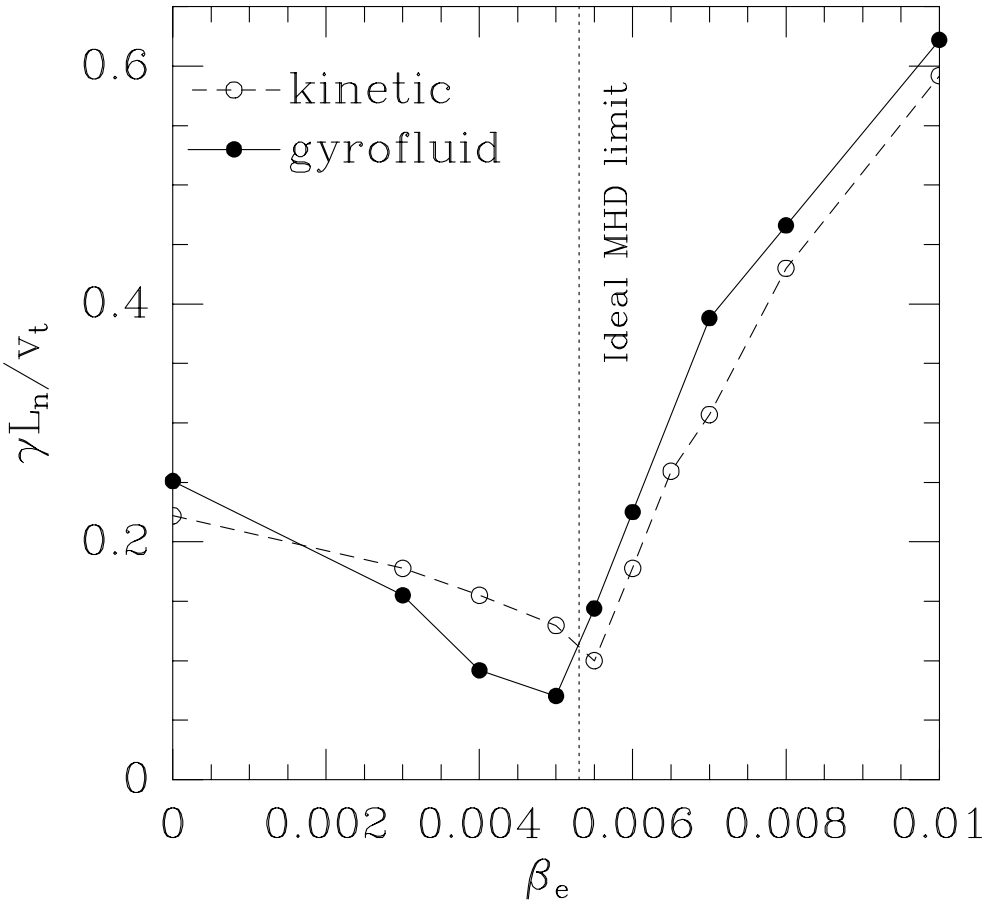

Figure 2: Comparison of gyrofluid with gyrokinetic calculations of the growth rate vs. β, showing the transition from an ITG instability at low β to a kinetic ballooning mode above the ideal β limit.

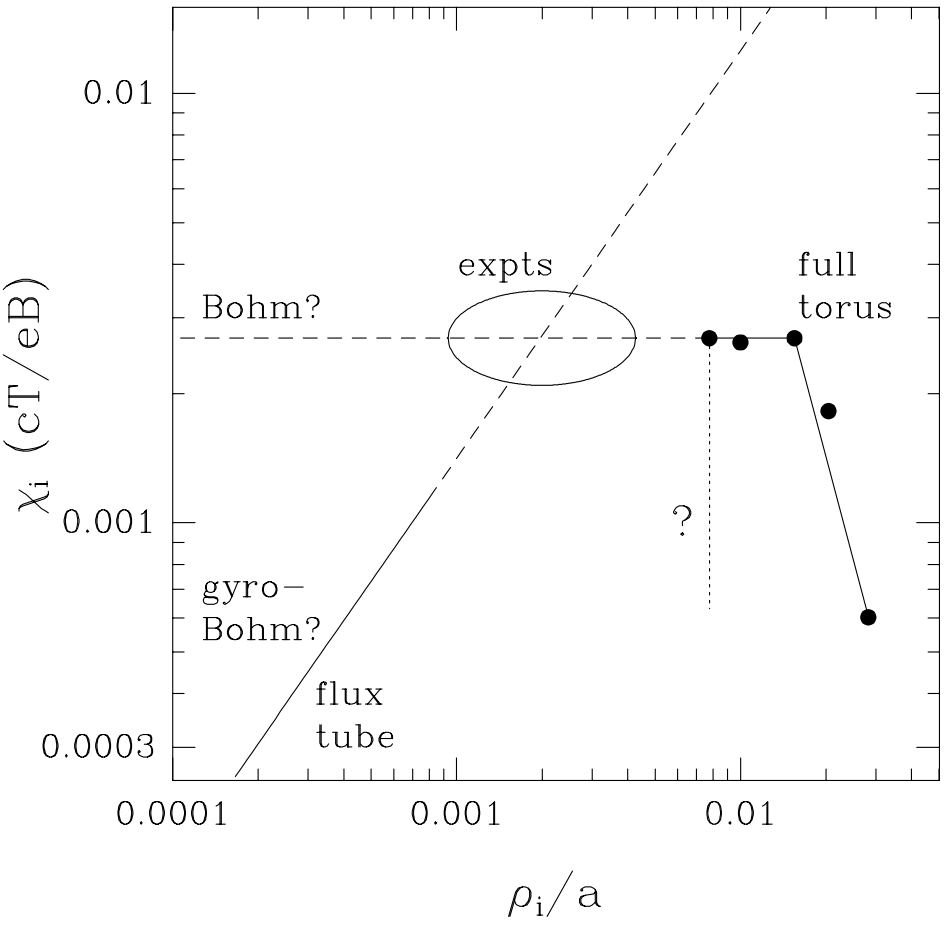

Figure 3: A conceptual illustration of the two scaling regimes observed for ITG-driven turbulence: Bohm scaling from the full-torus gyrokinetic code[38] at moderate ρ_*, and gyro-Bohm scaling in flux-tube codes in the limit $\rho_* \to 0$. The oval representing present experiments is not precise, and is meant only to illustrate the qualitative result that while dimensionless scaling experiments are closer to a Bohm than a gyro-Bohm scaling, there are recent encouraging comparisons of gyro-Bohm-type theories with a range of experiments[1]. One might conjecture that future tokamaks with smaller ρ_* will transition to a gyro-Bohm regime, but this is uncertain because the location and parametric dependence of the transition between these two regimes is not yet understood.